Self-organised states from solutions of active ring polymers in bulk and under confinement

Juan Pablo Miranda-López,[†,¶] Emanuele Locatelli,[*,‡,§] and Chantal Valeriani[*,†,¶]

† *Dep. Est. de la Materia, Física Térmica y Electrónica, Universidad Complutense de Madrid, 28040 Madrid, Spain*

‡*Department of Physics and Astronomy, University of Padova, 35131 Padova, Italy*

¶ *GISC - Grupo Interdisciplinar de Sistemas Complejos 28040 Madrid, Spain*

§*INFN, Sezione di Padova, via Marzolo 8, I-35131 Padova, Italy*

E-mail: emanuele.locatelli@unipd.it; cvaleriani@ucm.es

Abstract

In the present work we study, by means of numerical simulations, the structural and dynamical behaviour of a suspension of active ring polymers in bulk and under lateral confinement. At high activity, when changing the distance between the confining planes and the polymers' density, we identify the emergence of a self-organised dynamical state, characterised by the coexistence of slowly diffusing clusters of rotating disks and faster rings moving in between them. We further assess that self-organisation is robust in a range of polymer sizes and we identify a critical value of the activity, necessary to trigger cluster formation. This system has distinctive features resembling at the same time polymers, liquid crystals and active systems, where the interplay between activity, topology and confinement leads to a spontaneous segregation in an initially one-component solution.

1 Introduction

In the last few years, the study of active filaments and active polymers has attracted significant interest in the active matter community.[1] Active filaments are ubiquitous in Nature, ranging from the intra-cellular[2–4] to the extra-cellular[5–7] domains, encompassing unicellular[8–10] as well as complex multi-cellular[11–14] organisms. Active filaments are out-of-equilibrium due to the action of their fuel-consuming active units. Recently, artificial systems have been proposed,[15,16] harbouring promising technological applications.

It is well known that the structure of passive polymer fluids is influenced by many factors. Two of them that are often of key importance, especially in biophysics, are topology and confinement. Topology appears in multiple contexts ranging from DNA supercoiling,[17] to entanglements,[18] cyclisation[19] or supra-molecular linked materials.[20] Confinement is pivotal for polymers and biopolymers' organization, as well as for the development of intra-cellular active structures.[21] Notably, topology and confinement can give rise to unique structures, exemplified in the Kinetoplast DNA (or KDNA).[22,23]

On the active side, topology has not been given the same attention when dealing with suspensions of active filaments. While active ring models have been studied in very dilute[24–27] and in very dense[28,29] conditions, not much is known in between. Further, entanglements between active filaments may be relevant in the case of phase separation within a bulk suspension of worms[12,14]; yet, a only few modelling and theoretical works have been done so far.[30–32] Confinement has also been shown to play a key role in suspension of active particles. Active matter systems under confinement, such as micro-swimmers in narrow/corrugated channels,[33] bacteria moving through an asymmetric ratchet[34–37] or in soil[38,39] and epithelial layers,[40,41] have shown to exhibit a wealth of non-trivial properties.[42] In the case of active filaments, confinement has been employed to unravel features of chromatin dynamics.[3,4,43] However, with the exceptions of studies on very short polymer chains,[44,45] understanding the behaviour of active filaments under confinement is still far from complete.

For the above mentioned reasons, our goal is to study, numerically, the interplay between ac-

tivity, topology and confinement in a suspension of active ring polymers. In the last few years, different models have been proposed to describe bulk suspensions of active rings;[24–26,28] all models present an interesting and unique phenomenology. For our study, following Ref.,[27,46] we design activity as a polar (or tangential) force acting on each monomer (within the polymer). This active polymer model arguably displays the richest configurational and dynamical scenario at the single chain level.[27] When dealing with polar active polymers, non-equilibrium phenomena arise due to the interplay between activity and the local chain conformation. We foresee that the presence of several rings in the suspension and of a steric confinement will introduce further interplay, enriching the dynamical scenario.

By means of numerical simulations, we find that, under given conditions, the system displays a self-organised state, characterised by two populations of rings: clusters of slow active rings surrounded by a suspension of fast active rings. We demonstrate that this organisation appears at intermediate values of the monomer density and persist for several values of the separation between confining walls as well as in bulk conditions. Further, we show that ring size is a limiting factor: rings cannot be too long, otherwise collapse is inevitable, yet self-organisation is surprisingly lost if rings are too small. Finally, we show that self-organised clustering triggers rather abruptly at some value of activity.

The paper is structured as follows: in Section 2, we report the numerical model, the simulation details and the analysis tools. The results of the analysis are reported in Section 3. First, for rings of fixed size and high activity, we show in Section 3.1 how metric properties, such as the gyration radius and the prolateness of individual rings, i.e. their size and shape, averaged over the whole system, detect an heterogeneity at finite density. Next, we characterise the rings' clusters in Section 3.2, both in confinement and in bulk. Further, in Section 3.3, we use this information to demonstrate that, in the self-organised states, we distinguish two "populations" with different structural and dynamical properties: rings in clusters being larger and less mobile then outsiders. Finally, we discuss the effect of both ring length and activity: as mentioned, we demonstrate that self-organisation is robust in a window of values of the ring length and that it appears at a critical

value of the activity.

2 Model and Methods

Numerical model

Active polymer rings are modelled in a coarse-grained fashion, employing the well known bead-spring Kremer-Grest model.[47] Each polymer consists of N bonded active monomers. Monomers interact with each others via a repulsice WCA potential[48]

$$U^{\mathrm{WCA}} = \begin{cases} 4\varepsilon \left[(\sigma/r)^{12} - (\sigma/r)^{6} + \frac{1}{4} \right], & r < 2^{1/6}\sigma \\ 0, & \text{else} \end{cases} \tag{1}$$

where σ is the momoners' diameter, ε the unit energy. We set $\varepsilon = 50 k_B T$, k_B being the Boltzmann factor and T the absolute temperature.

Moreover, neighbouring monomers along the ring are held together by a FENE potential

$$U^{\mathrm{FENE}} = \begin{cases} -0.5 K R_0^2 \ln \left[1 - (r/R_0)^2 \right], & r \leq R_0 \\ \infty, & \text{else} \end{cases} \tag{2}$$

where we set K =30ε/σ^2=1500$k_B T/\sigma^2$ and $R_0 = 1.5\sigma$, being the latter each monomer diameter. This choice of parameters allows to avoid strand crossings, which would modify the unknot topology; particular care has to be taken in this respect.[27]

We introduce the polymer's activity in the form of a tangential self-propulsion force along the ring backbone. The active force $\mathbf{F}_i^{\mathrm{a}}$ with constant magnitude F_a acts on each monomer i: the force is directed along the vector $\mathbf{r}_{i+i} - \mathbf{r}_{i-i}$, parallel to the polymer backbone tangent.[46,49] Activity is quantified via the adimensional Péclet number, which measures the activity's strength in relation

to the thermal noise, defined as

$$\mathrm{Pe} = F_a \sigma / k_B T \tag{3}$$

where F_a is the modulus of the active force.

Simulation details

We study suspensions of unlinked and unknotted active ring polymers in bulk and confined between two parallel planes. A suspension consists of $M = 500 - 2000$ rings, each formed by a number of monomers N ranging from 32 up to 88; unless specified otherwise, we will focus on a specific ring size N =76. The rings obey to a Langevin Dynamics, simulated by means of the open source package LAMMPS,[50] with in-house modifications to implement the tangential activity. We integrate the equations of motion using the Velocity Verlet algorithm. Throughout the work, we consider a unitary mass; we further set σ and the thermal energy $k_B T$ as the units of length and energy, respectively, so that the characteristic simulation time τ is unitary. The friction coefficient γ is set to $1\tau^{-1}$. We choose time step $\Delta t = 10^{-4}\tau$ to prevent strand crossings.

We simulate suspensions of rings in bulk or under lateral confinement. In the former case, we employ periodic boundary conditions along the three directions. In the latter case, confinement is provided by two perfectly smooth, infinite planes, placed at a distance h and orthogonal to the z direction: the interaction between the flat walls and the monomers is purely repulsive, i.e. WCA-like, with $\sigma_w = \sigma$ and $\varepsilon_w = k_B T$. We consider suspensions characterised by different monomer densities $\rho = M \cdot N / V$, where V is the volume of the simulation box. In particular we consider ρ =0.05, 0.1, 0.2, 0.3, 0.4, 0.5, spanning from the dilute to the semi-dilute regime. In the confined case, we consider several values of the separation between confining plates, ranging from a tight confinement to the bulk case ($h/\sigma = \infty$): h/σ =3, 6, 9, 15, 21, 30.

The initial configurations are taken from well equilibrated suspension of unknotted, unlinked passive rings. Turning on the activity, we first perform equilibration runs 1) making sure (using Kymoknot[51]) that chain crossing does not occur at any time of the simulation and 2) computing

the linking number between any pair of neighbouring rings. After reaching the steady state, we perform production runs of (on average) $3-5\cdot10^5\tau$, corresponding to $3-5\cdot10^9$ time steps. For analysis purposes, snapshots of the systems are taken every $\tau_s = 10^3\tau$ or 10^7 time steps. For any given set of parameters, a single independent realisation of the system has been considered.

In order to choose the amount of activity the rings should experience, we take into account the fact that isolated short active rings in bulk are expected to undergo a swelling transition at sufficiently large Pe. This transition, in dilute conditions, is relatively sharp and the ring conformation is not affected by activity at low Pe. Thus, a suspension of active ring polymers significantly deviates from its passive counterpart only at high values of activity.[27] Thus, based on the previous study in dilute conditions, we set the limit of large activity at Pe=10. Moving to even larger values of the activity would require to set an even smaller time step, which would make the simulations extremely demanding. However, as mentioned, we explore the role of activity on self-organisation for two ring sizes.

Structural and dynamical analysis

In what follows, we are going to describe the tools we have used to characterise both structural and dynamical features of the suspension of active ring polymers in confinement and in bulk.

Structural properties of individual rings

To characterise the structural features of each polymer ring, we compute properties such as their gyration tensor, gyration radius and prolateness. The gyration tensor is defined as

$$G_{\alpha\beta} = \frac{1}{N}\sum_{i=1}^{N}\left(\mathbf{r}_{i,\alpha}-\mathbf{r}_{\mathrm{cm},\alpha}\right)\left(\mathbf{r}_{i,\beta}-\mathbf{r}_{\mathrm{cm},\beta}\right) \tag{4}$$

where the indices α and β run over the three Cartesian coordinates (x,y,z) of the N monomers of each ring, whose center of mass is $\mathbf{r}_{\mathrm{cm}} = \frac{1}{N}\sum_{i=1}^{N}\mathbf{r}_i$. The gyration radius of the rings can be

computed as

$$R_g = \sqrt{\lambda_1 + \lambda_2 + \lambda_3} \tag{5}$$

where $\lambda_1, \lambda_2, \lambda_3$ are the three eigenvalues of the gyration tensor. The shape of the rings is characterised computing the prolateness S, defined as

$$S = \left\langle \frac{(3\lambda_1 - I)(3\lambda_2 - I)(3\lambda_3 - I)}{I^3} \right\rangle \tag{6}$$

where $I = \lambda_1 + \lambda_2 + \lambda_3$. Depending on the values of S, the polymers' shape can be oblate (disk-like) or prolate (cigar-like): the shape is oblate if $S < 0$, isotropic (spherical) if $S \approx 0$ or prolate for $S > 0$.

Characterising active rings aggregation: clustering algorithm

In order to identify and highlight the self-organised structures that emerge in the polymer suspension, we perform a cluster analysis. First we compute the centre of mass (CM) of each polymer ring. We then perform a cluster analysis using the DBSCAN algorithm,[52] implemented in the Python library scikit-learn,[53] pre-computing the matrix of the mutual distances in order to correctly account for the periodic boundary conditions. This method allows us to detect clusters of different size, shape and polymer rings not belonging to any cluster (that we will name "outsiders"). Arbitrarily neglecting small clusters, we set the minimal number of elements in a cluster to be 5, and the cut-off distance d_{cut}, after performing several tests on all systems, to $d_{cut} = 4\sigma$ Since we are considering only the centre of mass of the polymer, we double check the results of the cluster analysis, assessing the identification of the clusters by visual inspection. Indeed, when cut-off values $d_{cut} > 4$ are employed, visibly distinguishable clusters started to merge while outsiders were classified as part of a cluster. Overall this classification resulted less precise. (see Supporting Information Sec.1 for more details on the parameter choice for the cluster analysis).

From the cluster analysis, we compute the average number of cluster N_c and the mean cluster fraction X, defined by the number of rings that form clusters divided by total number of rings. Both

quantities are averaged over time, when the system reached steady state.

Dynamical properties

The behaviour of the self-organised clusters has been highlighted analysing the clusters' dynamics. We focus on the clusters' "short" time behaviour, computing the absolute value of the displacement of the centre of mass of individual polymers in an interval $\tau_s = 1000\tau$

$$\Delta r = |\mathbf{r}_{\mathrm{cm}}(t+\tau_s) - \mathbf{r}_{\mathrm{cm}}(t)| \tag{7}$$

which corresponds to the sampling interval, reported in Section 2. Next, we evaluate the distribution of the displacements, distinguishing between rings that were, in both frames, part of a cluster from rings identified as outsiders. We choose this observable for two reasons. First, while clusters appear to be very long-lived, the individual rings can leave their cluster in the interval τ_s and, possibly, join other clusters. Further, clusters can merge in between frames. While it is possible, in principle, to keep track of the clusters in time, most rings join or leave a cluster. Thus, the statistics of long time displacements is rather poor. Second, this quantity is already sufficient to highlight the qualitative difference between rings belonging to clusters and outsiders.

3 Results and Discussion

3.1 Structural features of active ring polymers in bulk and confinement

We first evaluate structural properties such as the gyration radius and the prolateness, averaged over all rings and over time (in steady state). In Figure 1 we report both quantities for different values of confinement h/σ (y axis) and for suspensions at different densities (x axis). Each value of $(h/\sigma, \rho)$ corresponds to a simulation of a suspension of active ring polymers, each with N=76 monomers.

As shown in Figure 1, we observe the emergence of different behaviours. In panel a, upon

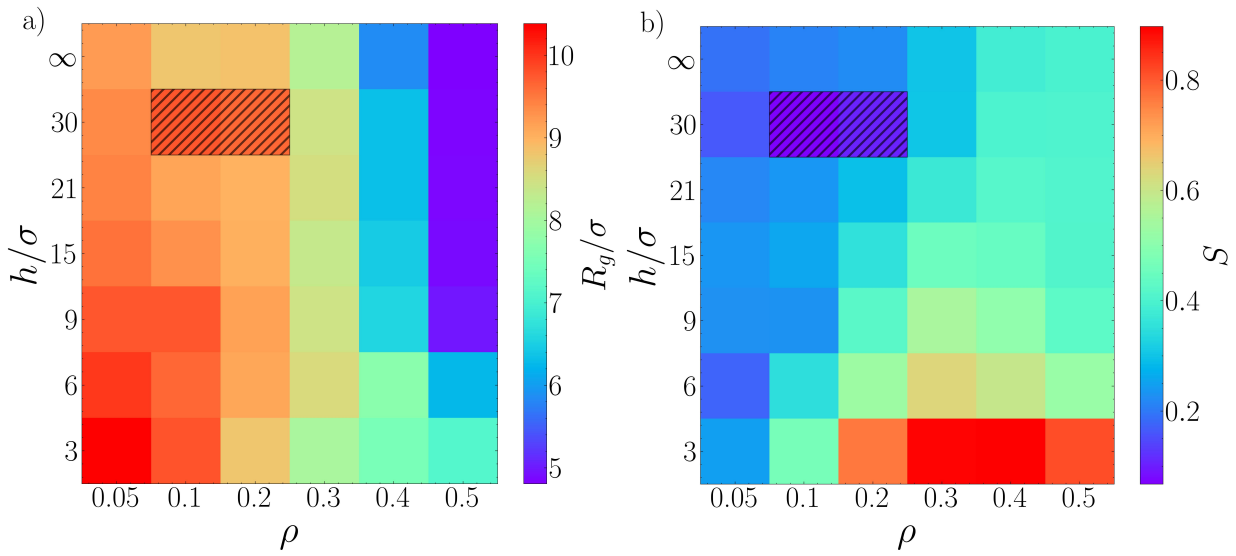

Figure 1: Colour plots of a) Mean gyration radius and b) mean prolateness for systems of active rings as a function of density ρ and lateral confinement h/σ. Each square corresponds to a simulation of a system of M =500 active ring polymers, each composed of N =76 monomers. The striped squares highlight results obtained simulating systems of M =2000 rings.

increasing the density and, similarly, upon increasing the separation between the confining planes, rings appear to shrink, i.e. the average gyration radius diminishes. In panel b, upon increasing ρ rings vary their shape from roughly spherical to prolate. However, upon increasing h/σ, S diminishes i.e. the rings' shape becomes more spherical. We underline that for two values of $(h/\sigma,\rho)$ (ρ =0.1, 0.2, h/σ =30) finite size effects were detected (striped squares in Figure 1). Thus, we had to perform additional runs with M =2000 rings.

The behaviours described in Figure 1 are qualitatively different from what is expected in suspensions of passive rings, and reflect the out-of-equilibrium nature of active polymer rings. In particular, passive rings would be expected to become more oblate, rather than prolate, when subject to very tight confinement, at least at sufficiently small density.[54] However, investigating the distributions of R_g and S across the range of densities, reported in Figure 2, we found that their average values, in most cases, were not representative of the ring population.

As shown in the top panels of Fig. 2), the peak of the R_g distribution is displaced, upon increasing the density, to lower values. This explains the average decrease observed in Fig.1. However, the distribution always spans the same, broad, interval of values. Remarkably, the distributions for

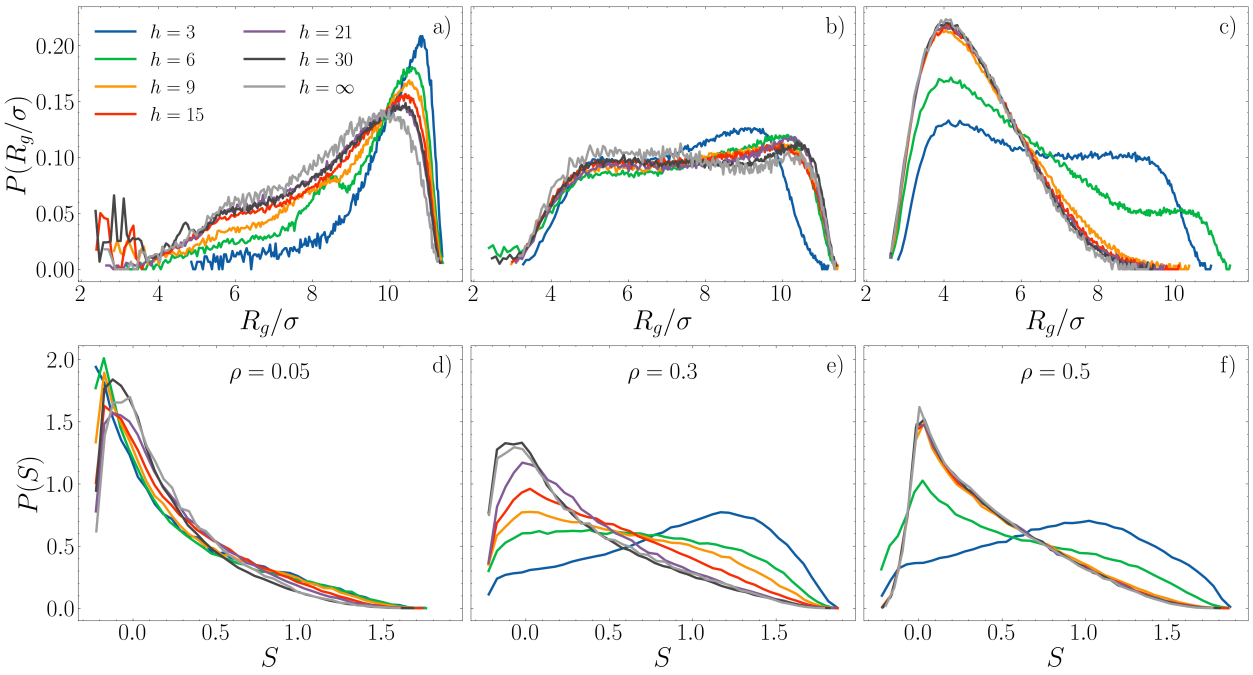

Figure 2: Distribution of R_g (top) and S (bottom) for density $\rho = 0.05$ (panels a,d), ρ =0.3 (panels b,e), ρ =0.5 (panels c,f) and several values of h/σ (as shown in the legend). The h values in the legend are in units of σ. The bulk system is reported as $h/\sigma = \infty$.

ρ =0.3 (panel b) are almost flat: a feature that is, in part, preserved at ρ =0.5 for the most confined cases (panel c). This implies that extreme conformations, compact or extended, are always present. Thus, the decrease of R_g observed in this work differs from the isolated case of either active linear or ring chains.[27,46]

As shown in the bottom panels of Fig. 2), the fact that rings appear spherical at low density emerges as the average of a very asymmetric distribution, presenting a peak at negative values of S and a fat tail extending to extreme prolateness values (panel d). Upon increasing the density (panel e), the peak of the distribution of S shifts towards S =0, i.e. the most probable conformation becomes quite spherical. However, the distribution maintains a long tail, which leads to an average positive prolateness (panels e,f). Finally, notice that the distribution becomes sensitive to the confinement at sufficiently large density: at h/σ=3 (dark blue line in panels e and f), its peak shifts to high positive values, signalling the preference of the rings to assume very elongated conformations.

All in all, the distributions of the gyration radius and of the prolateness suggest the presence of

an heterogeneous population of rings with different sizes and shapes.

3.2 The formation of active ring polymer ring clusters

To characterise the population heterogeneity emerging from the gyration radius and prolateness distributions of the rings' shape and size, we characterise the spontaneous formation of clusters. Interestingly, when systems are confined, the distinction between two different classes of rings (clustered and not clustered) emerges already by visual inspection. This is not the case for bulk systems, whose organisation is visually much less clear. For this reason, we will only show snapshots of confined systems.

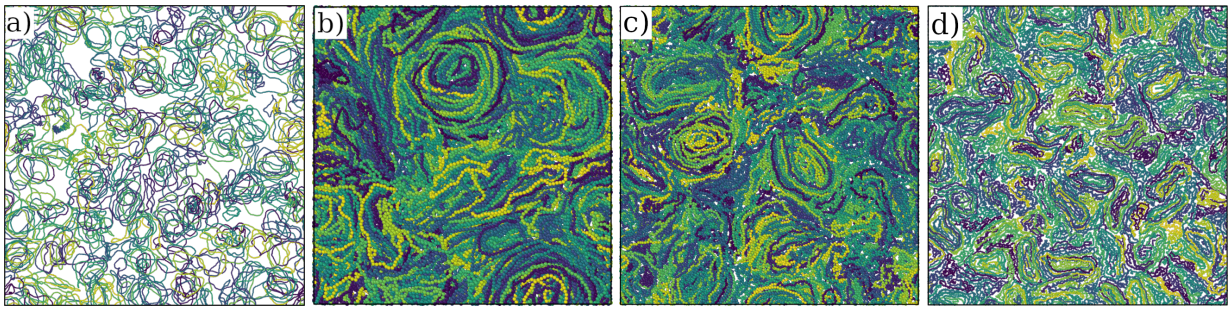

Figure 3: Snapshots of the top view of active rings suspensions (omitting the walls) for different values of ρ and h/σ. a) $\rho = 0.05$, $h/\sigma = 15$ represents a dilute case under tight confinement; b) $\rho = 0.3$, $h/\sigma = 21$ and c) $\rho = 0.4$, $h/\sigma = 9$ confined cases at intermediate density, where stacked rings are clearly visible; d) $\rho = 0.5$, $h/\sigma = 3$ the most dense and confined case. The colour code follows an arbitrary labeling of the rings and is only used to facilitate the visual distinction of individual chains.

Figure 3 reports the top view snapshots of active ring suspensions at different values of ρ and h/σ. Depending on the density and the confinement, rings undergo a process of self-organisation. Indeed, rings appear to arrange in peculiar conformations, not common in equilibrium suspensions of a passive polymer rings. In steady state, a fraction of the rings is arranged in nest-like structures or clusters. Within these clusters, the rings are rather flat and oblate(panels b,c) and, as dictated by the activity pattern, maintain a fairly steady rotation velocity (see videos in the Supporting Information). Notice that, given that they are visible from the top view, clusters are preferably located close to the confining walls. The remaining rings moves between clusters and take a more prolate

conformation. Notably, in order to form clusters, rings need a sufficiently high density (panels b,c) and space between confining planes to pile up. When the separation is large enough, clusters also form across the confining planes (panel a). One could assume that clustering is favoured at small separations, where it is easier to fill the space between planes with stacked rings, provided there is enough space. However, the most confined case considered here, h/σ =3 (panel d), is the one where the least amount of clustering and stacking is detected. Instead, in such a case, peculiar conformations of squeezed and elongated rings are favoured. While discussing the dynamics, we will highlight the sweet spot in the (ρ, Pe) plane, where confinement favours self-organisation (see Sec. 3.3).

We now focus on quantitatively characterising these self-organised states. In order to identify the self-organised clusters, we use the DBSCAN algorithm on the rings' centres of mass. The chosen cut-off distance, below which two rings are classified as neighbours, is $d_c = 4\sigma$, as reported in Section 2.

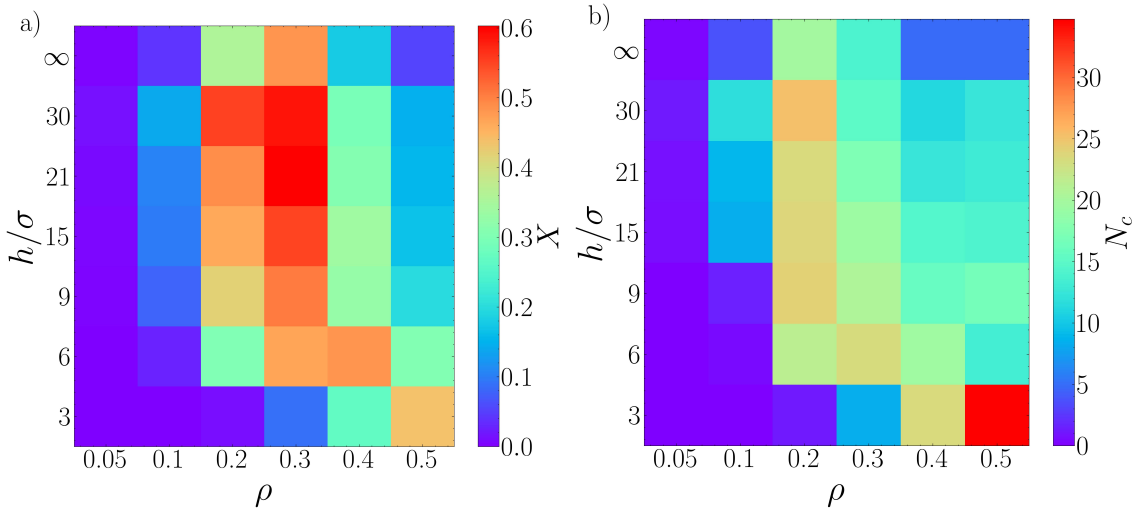

Figure 4: Colour plots of a) Fraction of rings belonging to a cluster X and b) mean number of clusters N_c for all simulated systems.

Figure 4 presents the cluster fraction X (panel a) and the mean cluster number N_c (panel b) as a function of the monomer density ρ and of the lateral confinement h/σ. Clearly, the clustering properties strongly depend on both density and confinement. At very high confinement, the algorithm detects clusters only at high density (see Supporting Information Sec.1). Indeed at

ρ =0.5, h/σ =3 we observe a significant amount of rings classified in clusters. These clusters are, naturally, numerous, as stacks cannot be populated by more than a few rings (see Fig. 5c).

At separations larger than h/σ =3, the simplest phenomenology appears at very low densities. Here, few clusters are detected, independently of h/σ. Accordingly, the cluster fraction is low. The interactions between rings are rare and, since there is no attraction, only transient and small clusters can be formed: these are mostly not detected by the algorithm due to our choice of a minimum cluster size of 5 rings. In the rest of the discussion, we will thus not further consider the case $\rho = 0.05$, as no self-organisation is possible.

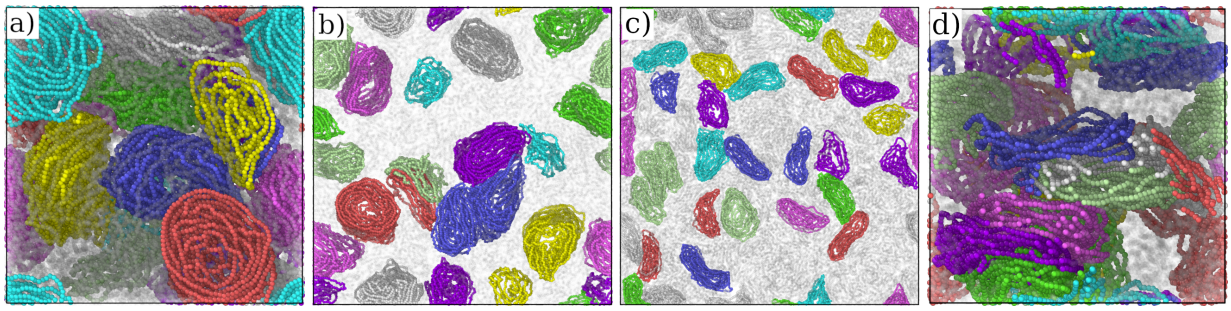

Figure 5: Snapshots of the active rings suspension, highlighting the ring self-organised clusters, for different values of ρ and h/σ. a) $\rho = 0.3$, $h/\sigma = 30$. b) $\rho = 0.4$, $h/\sigma = 6$. c) $\rho = 0.5$, $h/\sigma = 3$. d) $\rho = 0.2$ in the bulk. The systems under confinement are seen from the top, as in Fig. 3. The polymers labelled as outsiders are shown as transparent in order to highlight the clusters; different colours mark different clusters.

Upon increasing density, for h/σ >3, we notice a sharp growth in the cluster fraction, as well as in the number of clusters. These quantities reach a maximum value around $\rho = 0.2 - 0.3$ and, intriguingly, at large values of h/σ (see Fig. 5a). Figure 5d shows that such stacks are present also in the bulk, where there is no wall to "nucleate" the clusters: thus, their orientation is random. This makes them hard to detect, without a suitable algorithm. Upon further increasing the density, the cluster fraction and the number of clusters diminish. One would actually expect the opposite, as the system becomes denser. However, rings tend to assume more compact configurations, as noticed in Fig 2 and thus they cannot stack any more. The self-organisation is thus lost.

In order to provide an alternative way to measure the local organisation of the system, we compute the 2D radial distribution function $g(r)$ of the centre of mass, projecting their positions on the plane

orthogonal to the confinement (see Supporting Information Sec.2-4). Such a choice is dictated by the anisotropy of the system. The analysis confirms the results of the clustering algorithm at high activity and fixed N as well as, notably, upon varying N or Pe (Sec. 3.4, 3.5). Finally, an examination of the cluster fraction and the number of clusters as a function of the DBSCAN cut-off distance d_{cut} (see Supporting Information Sec. 1) further reveals that self-organising systems show strongly distinct features with respect to non self-organising or passive systems, for all values of d_{cut}. Thus clustering captures the features of the observed self-organisation. However, one needs to complement the cluster analysis with other observables to better unravel the consequences of said self-organisation.

3.3 Structure and dynamics of rings inside and outside of the clusters

From the snapshots reported in Fig. 5, it intuitively emerges that a straightforward way to characterise rings belonging to clusters with respect to outsiders consists of considering the difference in shape and size between the two groups. For this reason, we compute the distributions of R_g and S distinguishing between rings belonging to clusters and the outsiders.

When clusters are present, the distributions reported in Fig. 6 are markedly different. This can be observed in Fig. 6 a,c), reporting data for ρ =0.4, h/σ =6 (full lines) and $\rho = 0.3$, $h/\sigma = 30$ (dashed lines). On the one side, rings belonging to clusters tend to be expanded and oblate, with a distribution that usually has a peak at high values of R_g (panel a). On the contrary, outsiders rings tend to be prolate and present a more heterogeneous distribution of sizes, peaked at smaller values of R_g (panel b). When clusters are not present, the distributions are very similar, as in Fig. 6 b,d), reporting data for ρ =0.5, h/σ =21. This analysis highlights the fact that clusters, detected at large values of ρ, are due to local density fluctuations and not to self-organization.

Finally, it is intriguing that clusters remains even if confinement is relatively small, i.e. at large values of h/σ. Indeed, as already mentioned, stacks are present in the bulk. Figure 7 reports the distributions of R_g and S for rings classified as belonging to a cluster or as outsiders for systems in the bulk at different values of ρ.

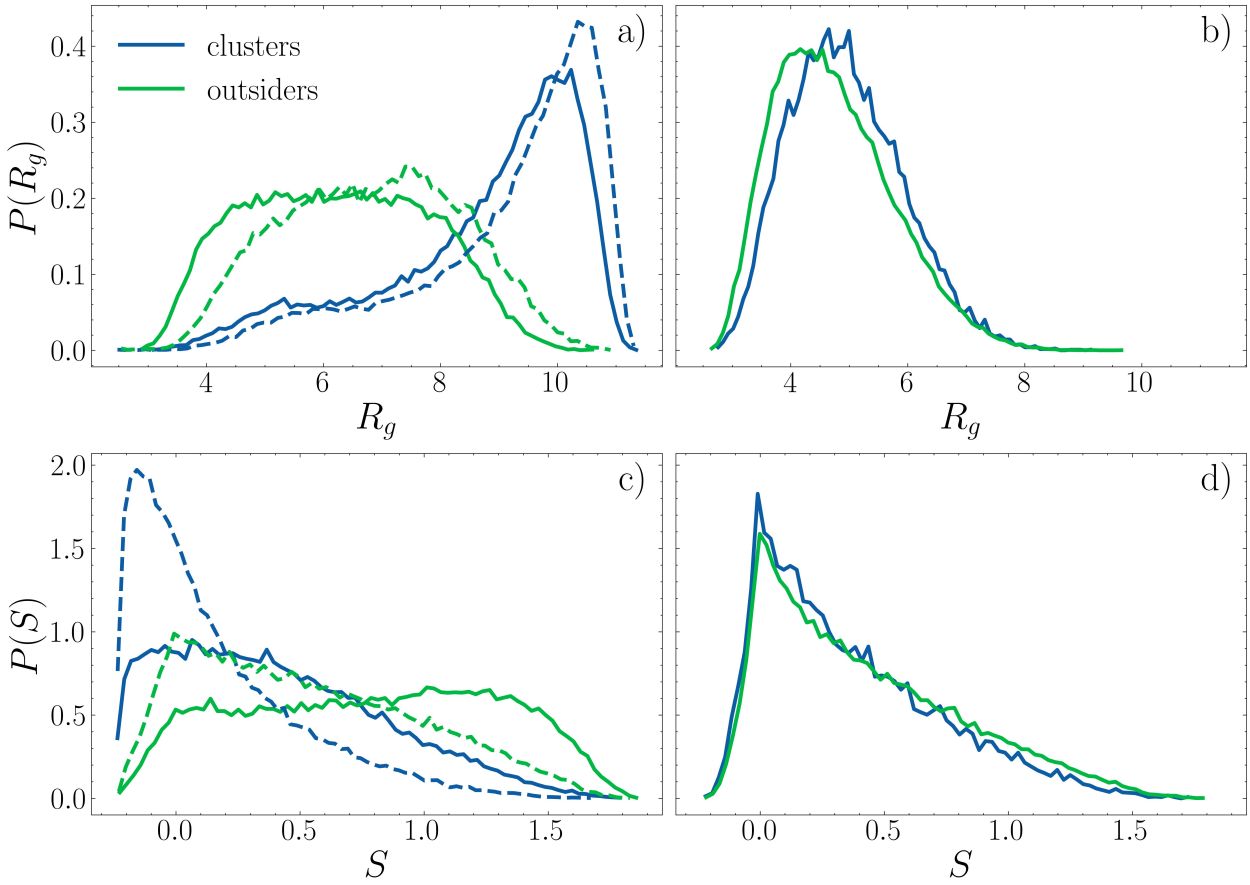

Figure 6: Probability distribution functions of R_g (panels a, b) and S (panels c, d) for rings detected as part of clusters (blue) or outsiders (green). Panels a, c report $\rho = 0.4$, $h/\sigma = 6$ (full lines) $\rho = 0.3$, $h/\sigma = 30$ (dashed lines); panels b, d report ρ =0.5, h/σ =21.

The same phenomenology observed under confinement emerges also here, confirming that clusters of disk-like rings form in the bulk within the density interval $0.05 < \rho < 0.5$.

We employ a similar strategy to investigate the dynamics. We consider the dynamical properties of rings belonging to a clusters versus the dynamics of outsiders, separately, and compute, for both populations of rings, the distribution of displacements of individual rings (as detailed in Section 2). Figure 8 shows examples of such dynamical analysis.

We observe the same phenomenon found upon looking at the distributions of the rings' size and shape: the distribution of the rings' displacements inside the clusters and of the outsiders is markedly different (Fig. 8a) when self-organisation is present. Instead, when no self-organisation emerges, all rings have the same displacement distribution (Fig. 8b).

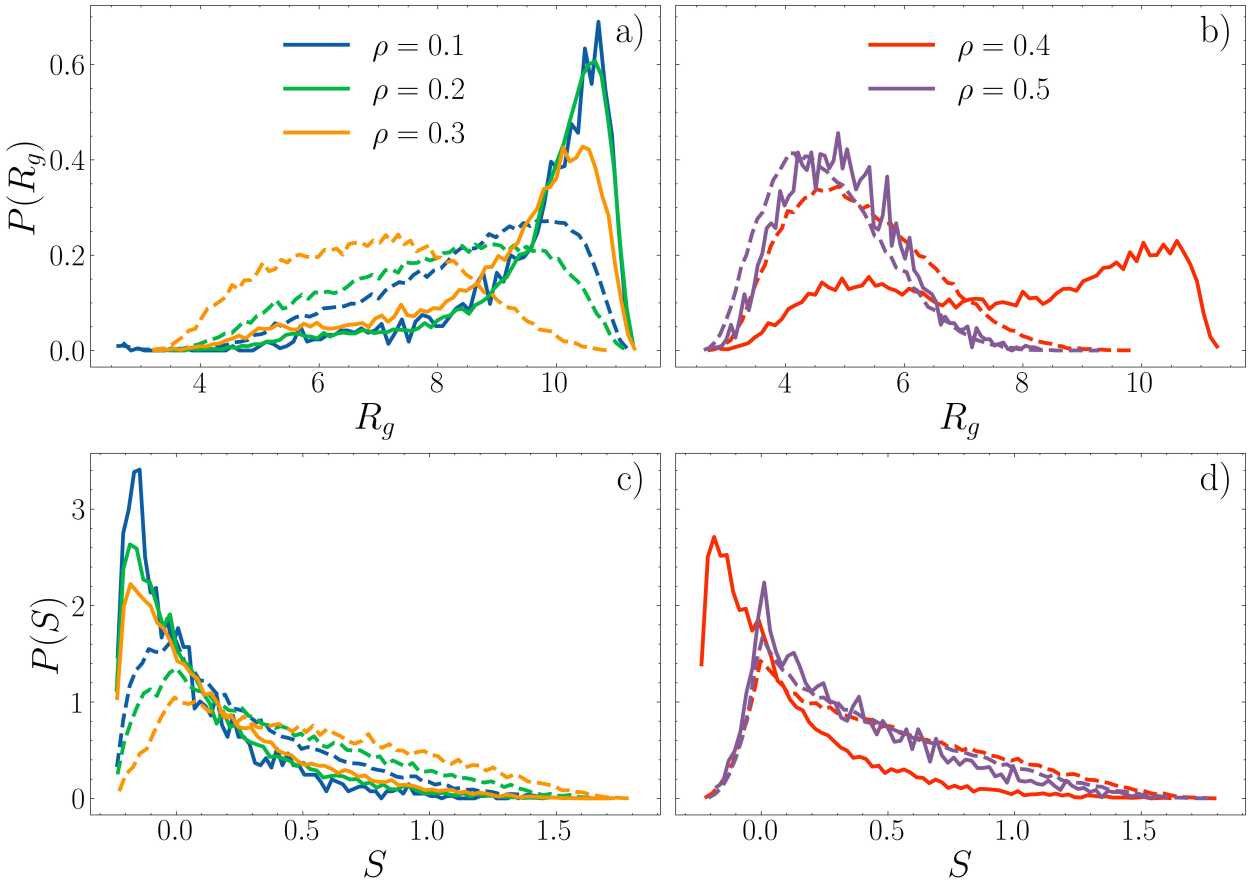

Figure 7: Probability distribution functions of R_g (panels a,b) and S (panels c,d) for active rings in the bulk at different values of ρ, detected as part of clusters (full lines) or outsiders (dashed lines).

In order to establish a more quantitative comparison between all systems, we extract, from the distributions in Fig.8, the most probable value of the displacement for rings belonging to clusters and outsiders, Δr_C and Δr_O, respectively. We report the results in Fig. 9, that can be understood when taking into account Fig. 4 and considering that it is not meaningful to consider systems where no clusters are present.

Thus, we leave blank spaces and focus on the rest of the phase diagram. By looking at the range of values reported in the two colorbars in Fig. 9a) and b), rings in clusters are less mobile than the outsiders. Counter intuitively, the mobility for rings in clusters increases upon increasing the density. The presence of the polar activity introduces a strong interplay between the polymer conformation and dynamics;[46] rings are more compact at high density and this enhances their mobility with respect to the swollen case. However, clusters at high density (ρ =0.5) are qualitatively

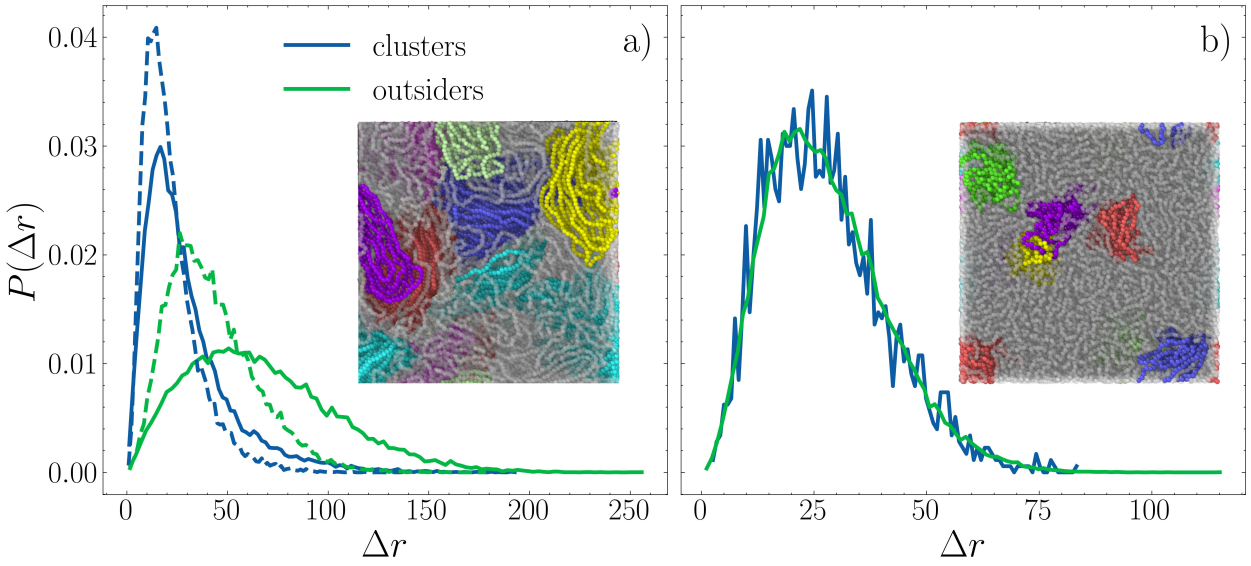

Figure 8: Probability distribution of the displacements $P(\Delta r)$ for rings belonging to clusters (blue line) and outsiders (green line). a) $\rho = 0.4$, $h/\sigma = 6$ (full line, snapshot in inset) $\rho = 0.3$, $h/\sigma = 30$ (dashed line) b) $\rho = 0.5$, $h/\sigma = 21$ (snapshot in inset). In the snapshots, outsiders are shown in grey, and the other colours highlight different clusters.

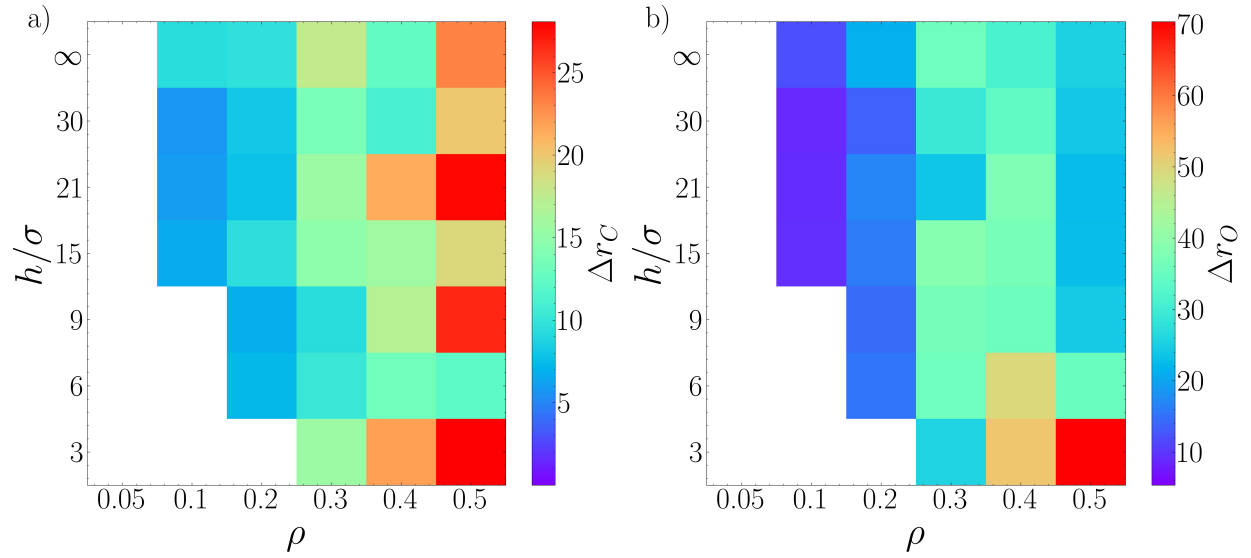

Figure 9: Colour plots of the most probable values of the displacements for (a) rings identified as part of aggregates, (b) ring identified as outsiders. The blank spaces highlight the system where the number of the identified clusters was negligible.

different from the ones at low density, as shown in the previous sections; thus, one should expect a change in their dynamical behaviour, due to the intimate connection between conformation and dynamics, typical of tangentially active polymers.

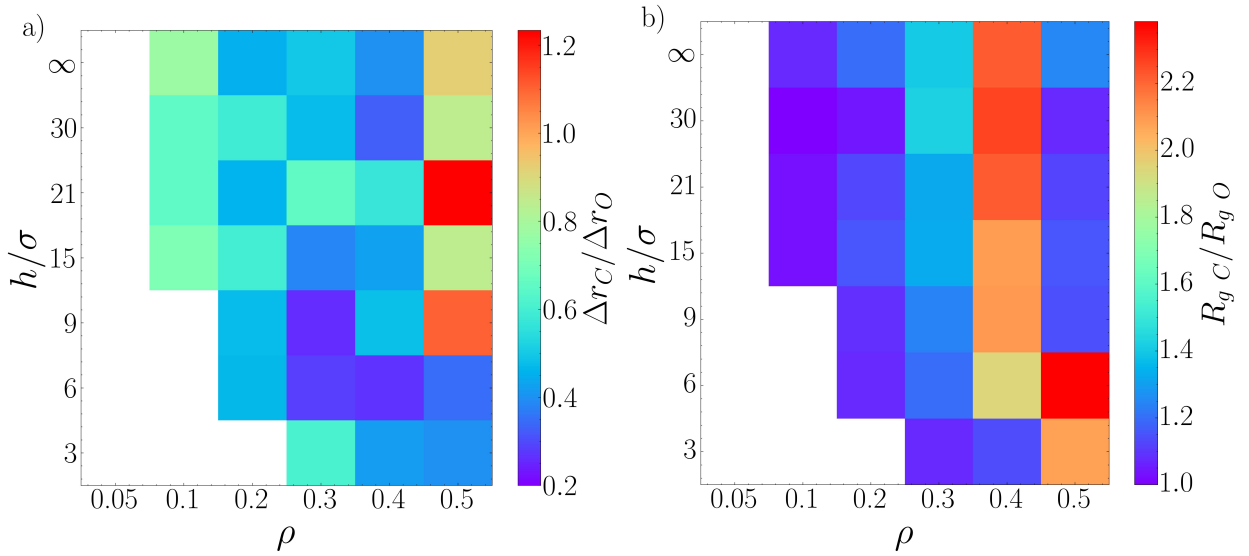

Figure 10: Color plots of the ratio between the most probable values of a) the displacements b) R_g, for rings in clusters and outsiders particles a function of the density ρ and the separation between the confining planes h/σ. The white colour highlights the system where the number of the identified clusters is negligible.

Finally, as a way to quantify the degree of heterogeneity within the two ring populations, we report in Fig. 10 the ratio between the most probable values of the observables computed so far, R_g and Δr, for rings inside C and outside O clusters: $R_{g,C}/R_{g,O}$ and $\Delta r_C/\Delta r_O$, indicated with subscripts C and O, respectively. When studying the displacements (panel a), it appears clear that systems with rings of different mobility are characterised by $\Delta r_C/\Delta r_O \ll 1$; otherwise $\Delta r_C/\Delta r_O \approx 1$. Instead, for the gyration radius (panel b), clusters are characterised by $R_{g,C}/R_{g,O} > 1$, or $R_{g,C}/R_{g,O} \approx 1$ otherwise. We underline, qualitatively, a correspondence between the two panels of Fig. 10: systems where clusters appear are also the systems where the size difference is more prominent. Finally, we highlight the two systems $\rho = 0.5$, h/σ =3 and $\rho = 0.5$, h/σ =6: these are the sweet spots, where confinement favours self-organisation when the system becomes denser (see also Fig 5c).

3.4 The effect of the active polymer ring size on the self-organisation mechanism

We now focus on the systems in which self-organisation is more evident, such as ρ =0.3 and h/σ =15; we compare it to a low density system $\rho = 0.05$, h/σ =15, to highlight the differences. Based on the ring behaviour at infinite dilution, one would expect self-organisation even for very short rings, characterised by small values of N. Interestingly, we will demonstrate that this is not the case in dense suspensions. We simulate systems of M =1000 active rings (to avoid finite size effects) of different length, ranging from N =32 to N =88, at the same activity value Pe = 10. The cluster analysis (cluster fraction X and the number of clusters N_c) is reported in Fig. 11, computed via DBSCAN with the same parameters as in Sec. 2. Further results for different values of d_{cut} are reported in the Supporting Information (Sec. 3).

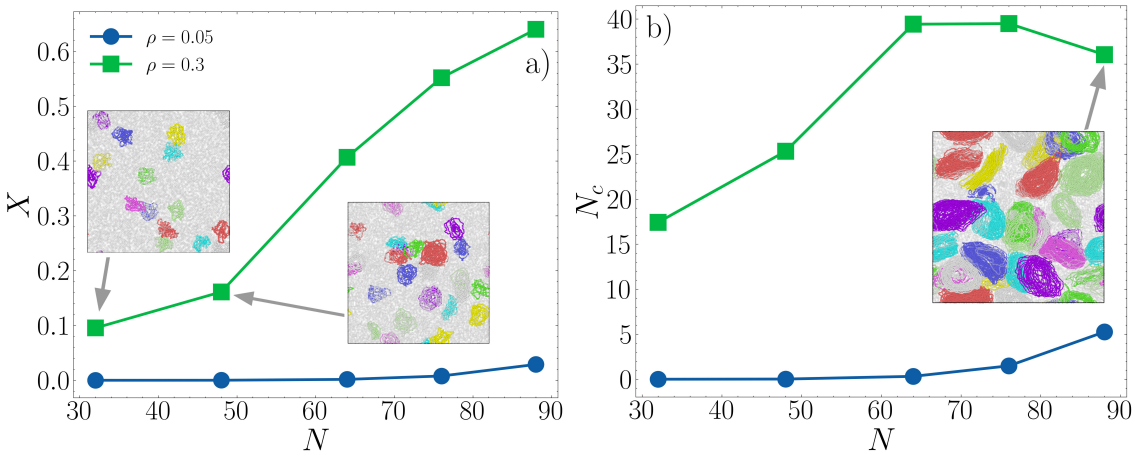

Figure 11: a) Cluster fraction X and b) number of clusters N_c as a function of the degree of polymerisation N for active rings at fixed value of the separation h/σ =15 and ρ =0.05 (blue circles), ρ = 0.3 (green squares). Lines are guides to the eye. Insets: snapshots of a) N =32 and N =48, b) N =88, as indicated by the grey arrows. outsiders are shown in grey, and the other colours highlight different clusters.

We observe that, at low density (blue circles), clustering is barely detected for all values of N, as expected. At ρ=0.3 (green circles), the cluster fraction X increases monotonically upon increasing N (panel a). The number of clusters N_c (panel b) shows a non-monotonic behaviour, with a peak around N =70 monomers per ring. From the dependency of X and N_c as function of

d_{cut} and from the distribution of the gyration radius inside and outside the clusters (Supporting Information, Sec. 3), we conclude that the smallest rings (N =32) do not self-organise in stacks. Upon increasing the ring size, the signatures of self-organisation becomes more and more evident until $N \approx 100$. For rings of that size, early signs of collapse, typical for large active rings,[27] appear and destroy the self-organisation (see Supporting Information Sec.3). We interpret these results in terms of the active rings "elasticity", i.e. their ability to recover the infinite dilution conformation after being perturbed by the presence of the other rings. In these terms, activity causes shorter rings to be less elastic than longer rings. On the one hand, this is counter-intuitive, since smaller rings should be quite rigid at infinite dilution and, having less degrees of freedom, they should be harder to perturb than longer rings. On the other hand, following Ref.,[27] the infinite dilution scaling $R_g \propto N$ implies that the activity-induced effective persistence length is increasing upon increasing N, as also suggested by the analysis of the bond-bond correlation function, reported in Ref.[27] In the very dilute limit, oblate conformations are stable for longer rings (up to $N \simeq$100) that are thus characterised by a larger effective persistence length. The results at finite density reported here are in agreement with such a scenario.

3.5 The effect of activity on the self-organisation mechanism

Finally, we discuss how increasing the activity of the single monomers from Pe = 0 to Pe = 10 affects self-organisation. The cluster analysis (cluster fraction X and the number of clusters N_c) is computed for M =1000 rings of length $N = 76$ and $N = 32$ and $0 <$ Pe < 10, and reported in Fig. 12. Clusters are computed via DBSCAN with the same parameters as in Sec. 2. Further results for different values of d_{cut} are reported in the Supporting Information (Sec. 4).

We focus again on systems in which the self-organisation is more evident, ρ =0.3, h/σ =15 and we compare to a low density system $\rho = 0.05$, h/σ =15. The low density case shows, for both values of N, no signs of clustering and self-organisation. Instead, the case $\rho = 0.3$ shows a remarkable behaviour. For N =76, the fraction of rings involved in clusters X increases abruptly at Pe =5 and stabilises for larger values of Pe. The number of clusters N_c also increases upon

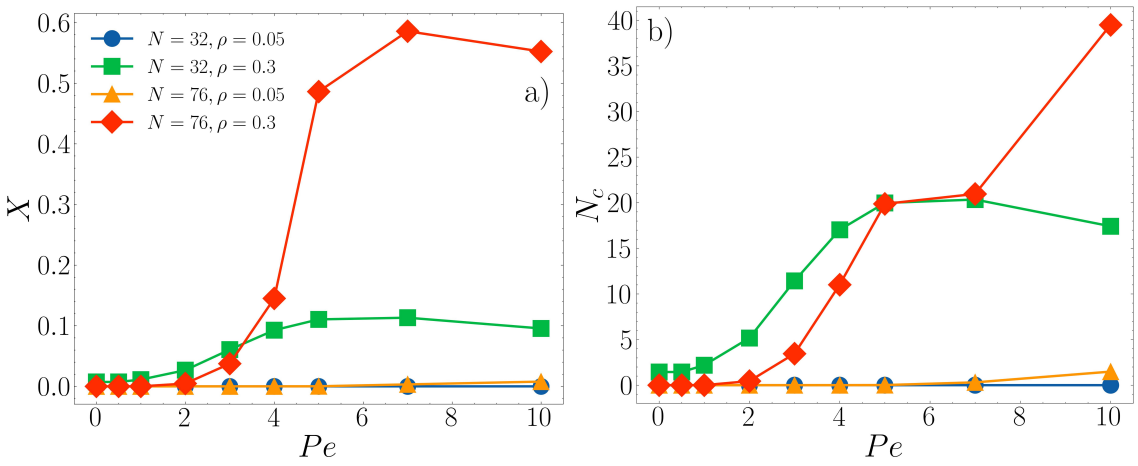

Figure 12: a) Radius of gyration R_g, b) cluster fraction X and c) number of clusters N_c as a function of the Péclet number Pe at fixed value of the separation h/σ =15 for N =32, $\rho = 0.05$ (blue circles) N =32, $\rho = 0.3$ (green squares), N =76, $\rho = 0.05$ (orange triangles), N =76, $\rho = 0.3$ (red diamonds). Lines are guides to the eye.

increasing Pe; however, it does not show such an abrupt increase, displaying, instead, a plateau, before a final increase at Pe =10. One can depict the following scenario: increasing the activity favours the emergence of larger clusters, containing more rings, until the activity is too high and smaller, more numerous clusters are favoured. The corresponding curves for N =32 showcase the radically different behaviour of a system where no self-organisation is present.

4 Conclusions

In our work, we have explored the conformation and dynamics of short active polymer rings in bulk and under confinement. We found quite a large ρ-h/σ parameter space where rings self-organised in clusters. Cluster formation happened not only under confinement (close to the walls) but also in the bulk (even though less prominently). We have further assessed lower and upper bounds for the ring size N as well as a lower bound for the activity, within which the self-organisation phenomenon is robust. It is possible to ascribe the origin of cluster formation to the combination of self-propulsion and the molecular fingerprint of rings.

Isolated short active rings tend to assume a swollen, disk-like configuration; this was associated

to an effective persistence length and to an effective "semi-flexibility".[27] In passive systems, semi-flexible rings have been reported to form clusters at high density.[55,56] However, there is a more delicate interplay here to consider. On the one hand, the presence of other active rings perturbs the disk-like conformation observed at infinite dilution, that results from the interplay between active forces, elasticity of the backbone and fixed topology. The activity is, in turn, connected to the polymer conformation; when the latter is perturbed, the action of active forces give rise to complex configurational rearrangements. Thus, the emergence of clusters in bulk is not trivial and rather unexpected. Intuitively, the self-organisation scenario is bound to fail at sufficiently high density, when the inter-chain contacts become dominant.

In addition to this, when considering the system under confinement, the molecular fingerprint of the rings is even more subtle. Passive ring polymer solutions under confinement have been shown to display an inhomogeneous density profile at relatively low density, with a marked tendency to accumulate to walls. Even in the passive case, oblate configurations are enhanced close to a wall.[54] Further, active agents interacting with walls display very distinct emergent patterns, which would not be present in equilibrium;[42] distinctively, they accumulate against walls.[34,42] Thus, the emergence of the stacks close to the walls becomes favourable from multiple perspectives: rings can remain in their most favourable configuration, which is indeed enhanced by the presence of the walls and wall accumulation is favoured, as rings can be packed more efficiently. Thus, when h/σ is large, rings have two mechanisms to stack: the "bulk" one, i.e. they pile up among themselves in a random orientation and the confined one, i.e. they pile up perpendicularly to the confining wall. This rationalises the excess of clustering and self-organisation observed even at quite large separation when, looking at the whole system, one sees little difference between bulk and confined distributions. We mention here that Ref.[10] reports on the self-organisation of Malaria sporozites in the salivary glands of a mosquito; intriguingly, the organisation observed in Ref.[10] resembles the one observed in this work, although the two systems are quite different. The sporosites are slender microswimmers, and were modeled as active linear polymer in “quasi” 2D, endowed with rigidity and chirality; here we have flexible unknotted rings in 3D, with no chirality. It is thus intriguing

to observe similar features, given the numerous differences. Further, a recent work[57] shows that clustering emerges also if different self-propulsion models at lower dimensionality are considered; at variance with this paper, the activity-induced clustering is there hindered by the polymer connectivity and topology.

Our computational study demonstrates the possibility of realising self-organising active fluids with polymers, where the peculiar "two population" fluid emerges thanks to the deformability and elasticity of the rings, that can switch between squeezed, elongated and swollen, disk-like configurations reversibly, without changing their topology. This system indeed shows features, typical of a liquid crystal, as the stacks may be seen as local regions of nematic order. Future work plans to investigate these features in more details. Further, it will be interesting to understand how to enhance or suppress self-organisation. The latter property may be relevant to biological systems such as the aforementioned malaria sporozites[10] and may be exploited as a mechanism to stop cells' development in a more focused and environmentally sustainable fashion.

Acknowledgement

J.P. Miranda acknowledges support by a STSM Grant from COST Action CA17139 (eutopia.unitn.eu) funded by COST (www.cost.eu). E. Locatelli acknowledges support from the MIUR grant Rita Levi Montalcini and from the HPC-Europa3 program. C.V acknowledges funding from MINECO grants C.V. acknowledges fundings EUR2021-122001, PID2019-105343GB- I00, IHRC22/00002 and PID2022-140407NB-C21 from MINECO. The computational results presented have been achieved using the Vienna Scientific Cluster (VSC) and the Barcelona Supercomputing Center (BSC-Marenostrum); CloudVeneto is also acknowledged for the use of computing and storage facilities.

Supporting Information Available

The following Supporting Information is available free of charge at the ACS website Video S1. Short video (top view) of a system of confined rings at $\rho = 0.3$ and $h/\sigma = 30$. Video S1. Short video (perspective view) of the same system of confined rings at $\rho = 0.3$ and $h/\sigma = 30$. Supporting Information text: additional information on the DBSCAN algorithm, the radial distribution function, the effect of the ring size and of the activity on the self-organisation.

References

(1) Winkler, R. G.; Gompper, G. The physics of active polymers and filaments. *The Journal of Chemical Physics* **2020**, *153*, 040901.

(2) Fletcher, D. A.; Mullins, R. D. Cell mechanics and the cytoskeleton. *Nature* **2010**, *463*, 485–492.

(3) Saintillan, D.; Shelley, M. J.; Zidovska, A. Extensile motor activity drives coherent motions in a model of interphase chromatin. *Proceedings of the National Academy of Sciences* **2018**, *115*, 11442–11447.

(4) Mahajan, A.; Yan, W.; Zidovska, A.; Saintillan, D.; Shelley, M. J. Euchromatin activity enhances segregation and compaction of heterochromatin in the cell nucleus. *Physical Review X* **2022**, *12*, 041033.

(5) Loiseau, E.; Gsell, S.; Nommick, A.; Jomard, C.; Gras, D.; Chanez, P.; D'ortona, U.; Kodjabachian, L.; Favier, J.; Viallat, A. Active mucus–cilia hydrodynamic coupling drives self-organization of human bronchial epithelium. *Nature Physics* **2020**, *16*, 1158–1164.

(6) Elgeti, J.; Gompper, G. Emergence of metachronal waves in cilia arrays. *Proceedings of the National Academy of Sciences* **2013**, *110*, 4470–4475.

(7) Chakrabarti, B.; Fürthauer, S.; Shelley, M. J. A multiscale biophysical model gives quantized metachronal waves in a lattice of beating cilia. *Proceedings of the National Academy of Sciences* **2022**, *119*, e2113539119.

(8) Balagam, R.; Igoshin, O. A. Mechanism for collective cell alignment in Myxococcus Xanthus bacteria. *PLoS Computational Biology* **2015**, *11*, e1004474.

(9) Faluweki, M. K.; Goehring, L. Structural mechanics of filamentous cyanobacteria. *Journal of the Royal Society Interface* **2022**, *19*, 20220268.

(10) Patra, P.; Beyer, K.; Jaiswal, A.; Battista, A.; Rohr, K.; Frischknecht, F.; Schwarz, U. S. Collective migration reveals mechanical flexibility of malaria parasites. *Nature Physics* **2022**, *18*, 586–594.

(11) Deblais, A.; Woutersen, S.; Bonn, D. Rheology of entangled active polymer-like T. Tubifex worms. *Physical Review Letters* **2020**, *124*, 188002.

(12) Deblais, A.; Maggs, A.; Bonn, D.; Woutersen, S. Phase separation by entanglement of active polymerlike worms. *Physical Review Letters* **2020**, *124*, 208006.

(13) Nguyen, C.; Ozkan-Aydin, Y.; Tuazon, H.; Goldman, D. I.; Bhamla, M. S.; Peleg, O. Emergent collective locomotion in an active polymer model of entangled worm blobs. *Frontiers in Physics* **2021**, *9*, 734499.

(14) Patil, V. P.; Tuazon, H.; Kaufman, E.; Chakrabortty, T.; Qin, D.; Dunkel, J.; Bhamla, M. S. Ultrafast reversible self-assembly of living tangled matter. *Science* **2023**, *380*, 392–398.

(15) Ozkan-Aydin, Y.; Goldman, D. I.; Bhamla, M. S. Collective dynamics in entangled worm and robot blobs. *Proceedings of the National Academy of Sciences* **2021**, *118*, e2010542118.

(16) Zheng, E.; Brandenbourger, M.; Robinet, L.; Schall, P.; Lerner, E.; Coulais, C. Self-Oscillation and Synchronization Transitions in Elastoactive Structures. *Physical Review Letters* **2023**, *130*, 178202.

(17) van Loenhout, M. T.; De Grunt, M.; Dekker, C. Dynamics of DNA supercoils. *Science* **2012**, *338*, 94–97.

(18) Everaers, R.; Sukumaran, S. K.; Grest, G. S.; Svaneborg, C.; Sivasubramanian, A.; Kremer, K. Rheology and Microscopic Topology of Entangled Polymeric Liquids. *Science* **2004**, *303*, 823–826.

(19) Haque, F. M.; Grayson, S. M. The synthesis, properties and potential applications of cyclic polymers. *Nature Chemistry* **2020**, *12*, 433–444.

(20) Hart, L. F.; Hertzog, J. E.; Rauscher, P. M.; Rawe, B. W.; Tranquilli, M. M.; Rowan, S. J. Material properties and applications of mechanically interlocked polymers. *Nature Reviews Materials* **2021**, *6*, 508–530.

(21) Marenduzzo, D.; Micheletti, C.; Orlandini, E. Biopolymer organization upon confinement. *Journal of Physics: Condensed Matter* **2010**, *22*, 283102.

(22) Chen, J.; Rauch, C. A.; White, J. H.; Englund, P. T.; Cozzarelli, N. R. The topology of the kinetoplast DNA network. *Cell* **1995**, *80*, 61–69.

(23) He, P.; Katan, A. J.; Tubiana, L.; Dekker, C.; Michieletto, D. Single-molecule structure and topology of kinetoplast dna networks. *Physical Review X* **2023**, *13*, 021010.

(24) Mousavi, S. M.; Gompper, G.; Winkler, R. G. Active Brownian ring polymers. *The Journal of Chemical Physics* **2019**, *150*.

(25) Philipps, C. A.; Gompper, G.; Winkler, R. G. Dynamics of active polar ring polymers. *Physical Review E* **2022**, *105*, L062501.

(26) Kumar, S.; Thakur, S. Local Polar and Long-Range Isotropic Activity Assisted Swelling and Collapse Dynamics of an Active Ring Polymer. *Macromolecules* **2023**, *56*, 5229–5236.

(27) Locatelli, E.; Bianco, V.; Malgaretti, P. Activity-induced collapse and arrest of active polymer rings. *Physical Review Letters* **2021**, *126*, 097801.

(28) Smrek, J.; Chubak, I.; Likos, C. N.; Kremer, K. Active topological glass. *Nature Communications* **2020**, *11*, 26.

(29) Chubak, I.; Pachong, S. M.; Kremer, K.; Likos, C. N.; Smrek, J. Active Topological Glass Confined within a Spherical Cavity. *Macromolecules* **2022**, *55*, 956–964.

(30) Manna, R. K.; Kumar, P. S. Emergent topological phenomena in active polymeric fluids. *Soft Matter* **2019**, *15*, 477–486.

(31) Tejedor, A. R.; Ramirez, J. Reptation of Active Entangled Polymers. *Macromolecules* **2019**, *52*, 8788–8792.

(32) Tejedor, A. R.; Ramírez, J. Dynamics of entangled polymers subjected to reptation and drift. *Soft matter* **2020**, *16*, 3154–3168.

(33) Bisht, K.; Marathe, R. Rectification of twitching bacteria through narrow channels: A numerical simulations study. *Physical Review E* **2020**, *101*, 042409.

(34) Galajda, P.; Keymer, J.; Chaikin, P.; Austin, R. A wall of funnels concentrates swimming bacteria. *Journal of Bacteriology* **2007**, *189*, 8704–8707.

(35) Reichhardt, C.; Olson, C.; Hastings, M. Rectification and phase locking for particles on symmetric two-dimensional periodic substrates. *Physical Review Letters* **2002**, *89*, 024101.

(36) Angelani, L.; Costanzo, A.; Di Leonardo, R. Active ratchets. *Europhysics Letters* **2011**, *96*, 68002.

(37) Ten Hagen, B.; Wittkowski, R.; Takagi, D.; Kümmel, F.; Bechinger, C.; Löwen, H. Can the self-propulsion of anisotropic microswimmers be described by using forces and torques? *Journal of Physics: Condensed Matter* **2015**, *27*, 194110.

(38) Mattick, J. S. Type IV pili and twitching motility. *Annual Reviews in Microbiology* **2002**, *56*, 289–314.

(39) Henrichsen, J. Twitching motility. *Annual Review of Microbiology* **1983**, *37*, 81–93.

(40) Henkes, S.; Kostanjevec, K.; Collinson, J. M.; Sknepnek, R.; Bertin, E. Dense active matter model of motion patterns in confluent cell monolayers. *Nature Communications* **2020**, *11*, 1405.

(41) Morris, R. G.; Rao, M. Active morphogenesis of epithelial monolayers. *Physical Review E* **2019**, *100*, 022413.

(42) Bechinger, C.; Di Leonardo, R.; Löwen, H.; Reichhardt, C.; Volpe, G.; Volpe, G. Active particles in complex and crowded environments. *Reviews of Modern Physics* **2016**, *88*, 045006.

(43) Liu, K.; Patteson, A. E.; Banigan, E. J.; Schwarz, J. Dynamic nuclear structure emerges from chromatin cross-links and motors. *Physical Review Letters* **2021**, *126*, 158101.

(44) Kurzthaler, C.; Mandal, S.; Bhattacharjee, T.; Löwen, H.; Datta, S. S.; Stone, H. A. A geometric criterion for the optimal spreading of active polymers in porous media. *Nature Communications* **2021**, *12*, 7088.

(45) Theeyancheri, L.; Chaki, S.; Bhattacharjee, T.; Chakrabarti, R. Migration of active rings in porous media. *Physical Review E* **2022**, *106*, 014504.

(46) Bianco, V.; Locatelli, E.; Malgaretti, P. Globulelike conformation and enhanced diffusion of active polymers. *Physical Review Letters* **2018**, *121*, 217802.

(47) Kremer, K.; Grest, G. S. Dynamics of entangled linear polymer melts: A molecular-dynamics simulation. *The Journal of Chemical Physics* **1990**, *92*, 5057–5086.

(48) Weeks, J. D.; Chandler, D.; Andersen, H. C. Role of repulsive forces in determining the equilibrium structure of simple liquids. *The Journal of Chemical Physics* **1971**, *54*, 5237–5247.

(49) Foglino, M.; Locatelli, E.; Brackley, C.; Michieletto, D.; Likos, C.; Marenduzzo, D. Non-equilibrium effects of molecular motors on polymers. *Soft Matter* **2019**, *15*, 5995–6005.

(50) Plimpton, S. Fast parallel algorithms for short-range molecular dynamics. *Journal of Computational Physics* **1995**, *117*, 1–19.

(51) Tubiana, L.; Polles, G.; Orlandini, E.; Micheletti, C. Kymoknot: A web server and software package to identify and locate knots in trajectories of linear or circular polymers. *The European Physical Journal E* **2018**, *41*, 1–7.

(52) Ester, M.; Kriegel, H.-P.; Sander, J.; Xu, X. A Density-Based Algorithm for Discovering Clusters in Large Spatial Databases with Noise. Proceedings of the Second International Conference on Knowledge Discovery and Data Mining. 1996; p 226–231.

(53) Pedregosa, F.; Varoquaux, G.; Gramfort, A.; Michel, V.; Thirion, B.; Grisel, O.; Blondel, M.; Prettenhofer, P.; Weiss, R.; Dubourg, V.; Vanderplas, J.; Passos, A.; Cournapeau, D.; Brucher, M.; Perrot, M.; Duchesnay, E. Scikit-learn: Machine Learning in Python. *Journal of Machine Learning Research* **2011**, *12*, 2825–2830.

(54) Chubak, I.; Locatelli, E.; Likos, C. N. Ring polymers are much stronger depleting agents than linear ones. *Molecular Physics* **2018**, *116*, 2911–2926.

(55) Poier, P.; Bačová, P.; Moreno, A. J.; Likos, C. N.; Blaak, R. Anisotropic effective interactions and stack formation in mixtures of semiflexible ring polymers. *Soft Matter* **2016**, *12*, 4805–4820.

(56) Staňo, R.; Smrek, J.; Likos, C. N. Cluster Formation in Solutions of Polyelectrolyte Rings. *ACS Nano* **2023**, *17*, 21369–21382, PMID: 37729077.

(57) Theeyancheri, L.; Chaki, S.; Bhattacharjee, T.; Chakrabarti, R. Dynamic Clustering of Active Rings. *arXiv preprint arXiv:2311.10007* **2023**,

TOC Graphic

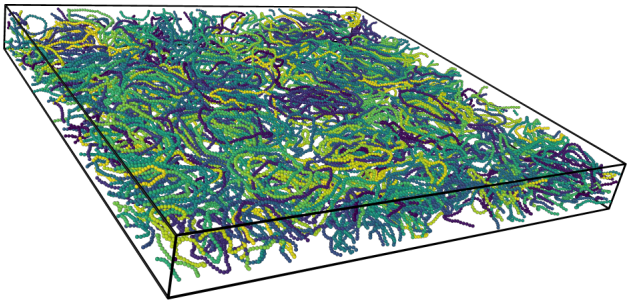

Snapshot of the system $\rho = 0.1$, $h/\sigma = 15$